POAC'11
Montréal, Canada

Proceedings of the 21st International Conference on
Port and Ocean Engineering under Arctic Conditions
July 10-14, 2011
Montréal, Canada

POAC11-035

NUMERICAL INVESTIGATION OF THE ICE FORCE DISTRIBUTION AROUND THE SHIP HULL IN LEVEL ICE

Junji Sawamura [1], Ryouhei Kikuzawa[1], Takashi Tachibana[1], Masaya Kunigita[1]

[1]Department of Naval Architecture and Ocean Engineering, Osaka University, Osaka, JAPAN

ABSTRACT

This paper investigates the ice breaking force distributions around a ship hull at the waterline when the ship advances in a level ice. This research forces on the ice bending failure and neglects the rotating and sliding force of the broken ice floes. The numerical simulation consists of two parts: 1) the repetitive ship-ice contact and 2) bending failure of the floating ice plate. Contact circles technique is adopted for the ship-ice contact detection. The contact conditions at the contact ice edge such as the crushing area is obtained by the geometrical conditions. The ice breaking process deals with a bending failure. A bending behavior of the floating ice is calculated by the finite element method of fluid-structural interaction. A large amount of FE simulations are carried out in various ship-ice contact conditions e.g. wedge angle, ice thickness and contact force. The ice breaking force and the length of a broken ice piece are efficiently obtained by the database of the ice bending behavior resulted from the FE simulations. The developed simulation can predict the ice force distribution and the number of the ship-hull contacts along the waterline. The simulations are performed in the ship head-on and turning maneuver with different bow forms, ship speed, turning radii and ice thicknesses. The relationship between the distributions of the ice force and ship-ice contact at the waterline is explained. The effect of the ship maneuvering conditions on the ice force distribution is discussed by the numerical results.

INTRODUCTION

For ship structural design and good maneuverability in an ice sea, to understand mechanism of procedure for ice load e.g. when, where and how big ice load acts on a ship structure, is vital issue. Most of the ice load predictions are still based on the full-scaled and experimental data. The numerical simulation based on the physical investigation should be needed. However, all of the studies related to predicting ice load are still unsatisfactory due to the complexity of the ice breaking mechanism with ship-ice interactions. In a ship operating in a level ice, the ship mainly breaks the level ice at the bow part where is optimized the hull shape for efficient icebreaking. On the other hand, in turning operation, a ship collides at the side hull and the aft area where is less icebreaking performance, therefore, occasionally causes massive damage to the structures. To estimate the ice load distribution around a ship hull in ship maneuvering in a level ice including a turning operation should be important.

Kayo, Y. (1993) and Liukkonen, S., et al., (1992) carried out an experiment using a segmented ship model to measure ice load distribution around a ship hull. The segmented model is suitable way to measure the ice load distributions. However, the number of segments is limited so that it's difficult to know detailed ice load distributions. Izumiyama, K. et al., (2001) measured detailed

ice force distributions by the model test installed a sheet-shaped pressure sensor, which can obtain 2 dimensional pressure data with high resolutions. The experiment with the pressure senor is more useful way than the segmented model test, but has not clarified detailed relationship between the ship-ice contact and the ice load distribution yet. The numerical simulation developed by physical investigation of the ice breaking process is seemed to be useful tool to estimate the complex ice load distributions. Valanto, P., (e.g. 2009) developed the sophisticated numerical simulations which can calculate the ice load distributions at the waterline. Liu et al., (2008) have developed the real time simulations of ship maneuvering in level ice. They have carried out significant work done by their developed numerical simulations. Authors also have studied on development of the numerical simulation to estimate ice load distributions in ship going into level ice (Sawamura, et al., 2008 and 2010).

The ice load consists of two phases: 1) the bending failure of the ice sheet, and 2) the rotating and sliding of broken ice floes. The ice bending induces a maximum force peak during the one cycle of the ice load. The force due to the rotating and sliding phase induces relatively smaller force after the ice bending failure occurs. This research focuses on the force peak due to bending and ignore the contributions of the broken ice pieces on the ice load. After ship-ice contact, the ice edge is crushed by the ship hull. The contact force is increasing with increasing crushing area. The crushing area depends on the ship-ice contact conditions such as the ship motion, ice thickness and so on. Sawamura, et al (2010) showed that the ship motion of the surge, sway and yaw described by 3DOF rigid body equation tends to make narrower ice channel and smaller ice force distributions than the constant ship motion. However, in this research, the ship motion with the constant direction and the speed is applied to investigate the relationship between the ship-ice contact conditions and the ice bending force distributions.

This paper investigates the ice force distributions around a ship hull when the ship advances in a level ice by authors developed numerical simulation. The simulation consists of two parts: 1) the repetitive ship-ice contact and 2) bending failure of an ice plate. A contact circle technique is applied to the repetitive ship-ice contact detections. Finite Element fluid-structural interaction is used to calculate a bending behavior of a floating ice plate. In order to make database of the ice bending failure, a large amount of the FE simulations in various ice-ship contact conditions such as ship speed, ice wedge angle and ice thickness are carried out. In the repetitive ship-ice interactions, the ice breaking force, the breaking time and the length of the broken ice at each contact edge are interpolated from the database of the FF simulations. In this research, the new database related to the ice thickness is added to the previous database (Sawamura, et al., 2010). The effect of the ice thickness on the ship-ice contact and the ice force distributions are investigated in addition to one of the ship speed, the turning radius and the bow shape. The numerical results show that the developed simulation has possibilities to understand detailed ice load mechanism and to estimate ice load distributions accurately and efficiently.

SIMULATION FOR SHIP

Ship-ice contact

When a ship advances into a level ice, the ship repeatedly contacts with the ice edge. The ice edge is broken off from the ice plate by the ice plate bending. During a ship maneuvering, there is a large amount of the ship-ice contacts so that the efficient contact detection should be needed to develop a numerical simulation. In this research, the circle contact detection is applied to ship-ice contact. Figure 1 shows schematic of the circle contact technique. The outlines of the ship hull

and the ice edge are expressed by a large amount of small circles. At the contact point, the following equation related to a distance between two circles of the ship and the ice is satisfied:

$$(x_i - x_s)^2 + (y_i - y_s)^2 = (r_i + r_s)^2 \ , \quad (1)$$

where (x_i , y_i) and (x_s , y_s) are x-y coordinate of the center of the ship and the ice circles, respectively. r_i and r_s are the radius of two circles, respectively. After detecting the contact point, a certain ice area which is the broke ice floe is deleted from the ice plate area. Then the ice circles are relocated along the outline of the new ice edge. The continuous contact process such as the ship-ice contact and the ice edge breaking during the ship maneuvering in the level ice can be calculated by this simple algorithm.

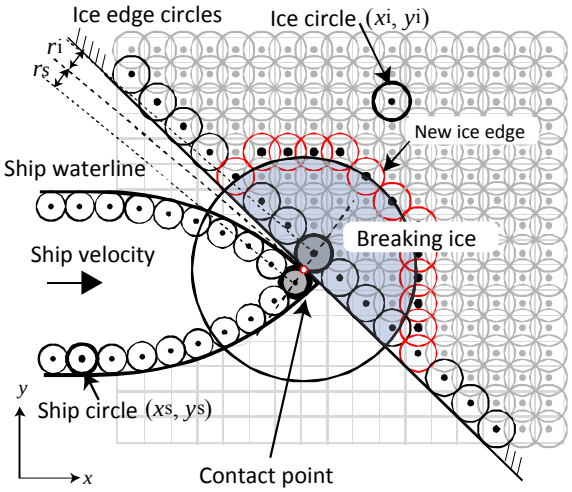

Figure 1. Contact circles applied to the ship-ice contact interactions.

Force component at contact surface

After the ship-ice contact, a level ice is pushed down by the ship advancing. At the same time, the ice edge is crushed by the ship hull, and the contact force increases with increasing the crushing area. A contact force is assumed to increase proportionally with the crushing area. The contact force in the normal direction on the contact surface is given by:

$$F_n = A_c \cdot \sigma_c \ , \quad (2)$$

where F_n is normal contact force, A_c is a crushing area and σ_c is compressive strength of the ice. A crushing area A_c depends on a geometrical condition at the contact edge such as a ship penetrating distance into an ice edge, ice thickness, ice wedge angle and ship hull angle. In this research, a crushing area is proportionally increasing with the ship penetrating time for simplicity of the numerical simulation. Detailed description to derive the relationship between the crushing area and the ship penetrating time into the ice edge is shown in Sawamura, et al., 2008. A friction force acts on the contact surface in the opposite direction to the relative motion between the ship hull and the ice contact plane. A friction force is described by following equation:

$$F_f = \mu \cdot F_n \ , \quad (3)$$

where F_f is a friction force, μ is a friction coefficient. A contact force F_{total} is calculated by sum of a contact force F_n and a friction force F_f.

Ice breaking

A level ice is broken by a bending failure. A bending behavior of the floating ice plate is significantly influenced by the fluid force induced by the water flow underneath the ice plate. In addition, a contact edge becomes a great variety of 3D wedged ice. In this research, the bending behavior of 3D wedged floating ice is calculated by FE fluid-structural interaction using ABAQUS/Explicit. A vertical component of the contact force F_{total} described by the equations (2)

and (3), which is related to the plate bending is given as the force boundary condition at the ice edge in the FE simulations. This vertical force acting on the ice edge in the FE simulations is assumed to be proportional to a ship penetrating time. A horizontal component which is related to the in-plane stress in the ice plate is ignored in the FE simulations.

In this paper, a bending failure occurs under following criterion: 1) A circular or an elliptical broken ice floe is usually observed in the model tests and the full-scale measurements. A circle shape is assumed to be an ice broken floe. 2) A bending failure occurs at the point where the surface stress on the ice plate exceeds a flexural strength of an ice. A circumferential crack immediately propagates from the occurring point of the bending failure. 3) For the wide wedged ice whose wedge angle is larger than 120°, the ice plate is divided into two plates by the radial crack along the center of the ice plate. Next, the circumferential crack occurs in the same manner of the narrow ice plate. A schematic of the bending failure is shown in Figure 2.

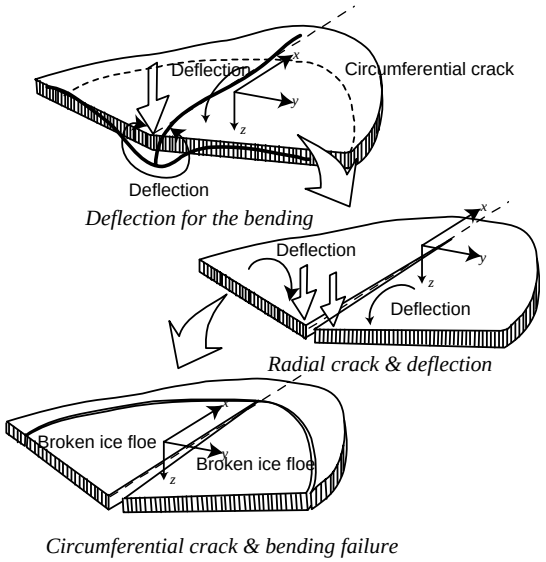

Figure 2. Bending failure of the ice plate with large wedge ice.

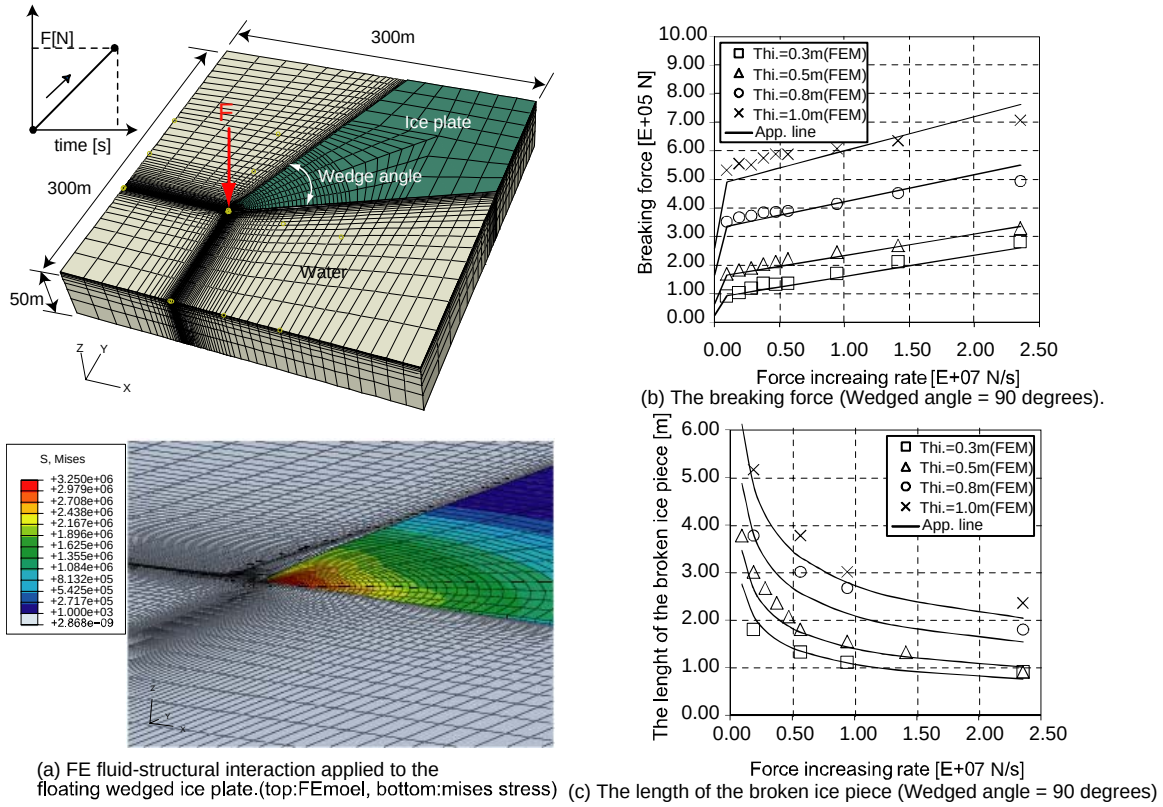

(a) FE fluid-structural interaction applied to the floating wedged ice plate.(top:FEmoel, bottom:mises stress)

(b) The breaking force (Wedged angle = 90 degrees).

(c) The length of the broken ice piece (Wedged angle = 90 degrees)

Figure 3. Examples of (a) FE model of fluid structural interaction and Mises stress, (b) the ice breaking force and (c) the length of the broken ice piece of FEMs and approximated lines.

At the bow where is lower hull angle, the vertical component in the contact force is dominant so that the ice plate is broken by the bending failure. On the other hand, at the shoulder where is steeper hull angle, the horizontal component is significantly increasing so that the ice plate might be broken by the other failure mode such as the ice buckling. In this paper, the bending failure in the ice plate is only considered for the ice breaking force. The contributions of the fluid flow induced by the ship advancing such as the ventilation are also ignored in the ice bending failure of the FE simulation.

A large amount of FE simulations in different ice conditions, e.g. the ice thickness, the wedge angle and the force increasing rate at the ice edge are carried out. The breaking force, the length of broken ice and the breaking time of the wedged ice in the repetitive ship-ice contact simulation are obtained by the database which results from the FE simulations. The ice is assumed to be homogenized material, whose Young's modulus E is 5.4 GN/m^2, Poisson ratio ν is 0.3, flexural strength σ_f is 1.0 MPa and compressive strength σ_c is 2.8 MPa. Friction coefficient μ is 0.1. In this research, the data related to ice thickness is added to the previous database. Figure 3 shows examples of the FE model, the breaking force and the length of the broken ice piece in different ice thickness as a function of the force increasing rate resulted from the FE simulations.

NUMERICAL RESULTS

Ice force in ship head-on maneuver

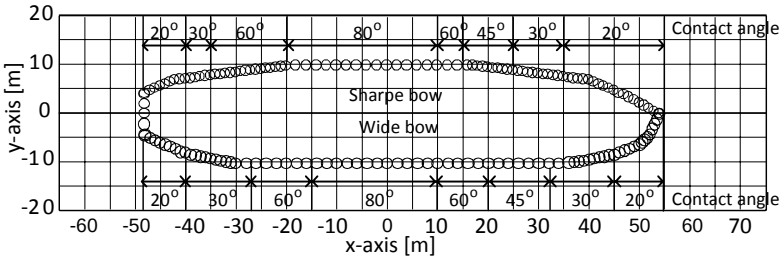

Figure 4. Virtual model ship for the simulations.

Figure 4 shows numerical ship models at the waterline. A virtual icebreaker model with a sharp bow (L × B =104×22m) as show in the top part of Figure 4 is used. The ice thickness is varied from 0.3m to 1.2 m. The ship speed is varied from 1.0 m/s to 5.0 m/s. The influence of an ice thickness and a ship speed on the average ice contact force in x (surge), y (sway) and z (heave)-direction and the length of the broken ice are investigated. Figures 5(a)-(c) show relationship between the ice thickness and the average ice contact force in the different ship speeds = 2.0, 3.0 and 5.0m/s. Figure 5(d) shows relationship between the ice thickness and the length of broken ice piece in different ship speeds from 1.0 to 5.0m/s. In Figures 5(a)-(c), the resistance force increases with increasing the ice thickness and the ship speed. In Figure 5(d), the length of the broken ice pieces increases with increasing ice thickness but decreasing the ship speed. These results show that the ice contact force at the contact point significantly increases with the ice thickness, and the average ice force increases with increasing the ship speed even decreasing the number of ship-ice contact which is caused by increasing the length of broken ice pieces. On the other hand, the ice contact force and the number of the ship-ice contact increase with ship speed, then the average ice force increases with the ship speed by synergistic effect of the ice contact force and the number of ship-ice contacts. The developed numerical simulation can explain the relationship between the ice contact force and the ship maneuvering conditions such as ice thickness and the ship speed. The irregular force peaks are observed in the conditions of 0.5m thickness and 2.0m/s ship speed (See Fig. 5(b)), and 0.8m thickness and 3.0m/s ship speed (See Fig. 5(b)). The irregular lengths of the ice piece are also observed in the same conditions as the 0.5m thickness and 2.0m/s ship speed (See Fig. 5(d)). This result implies the relationship between distributions of the ship-ice contact and the average ice force.

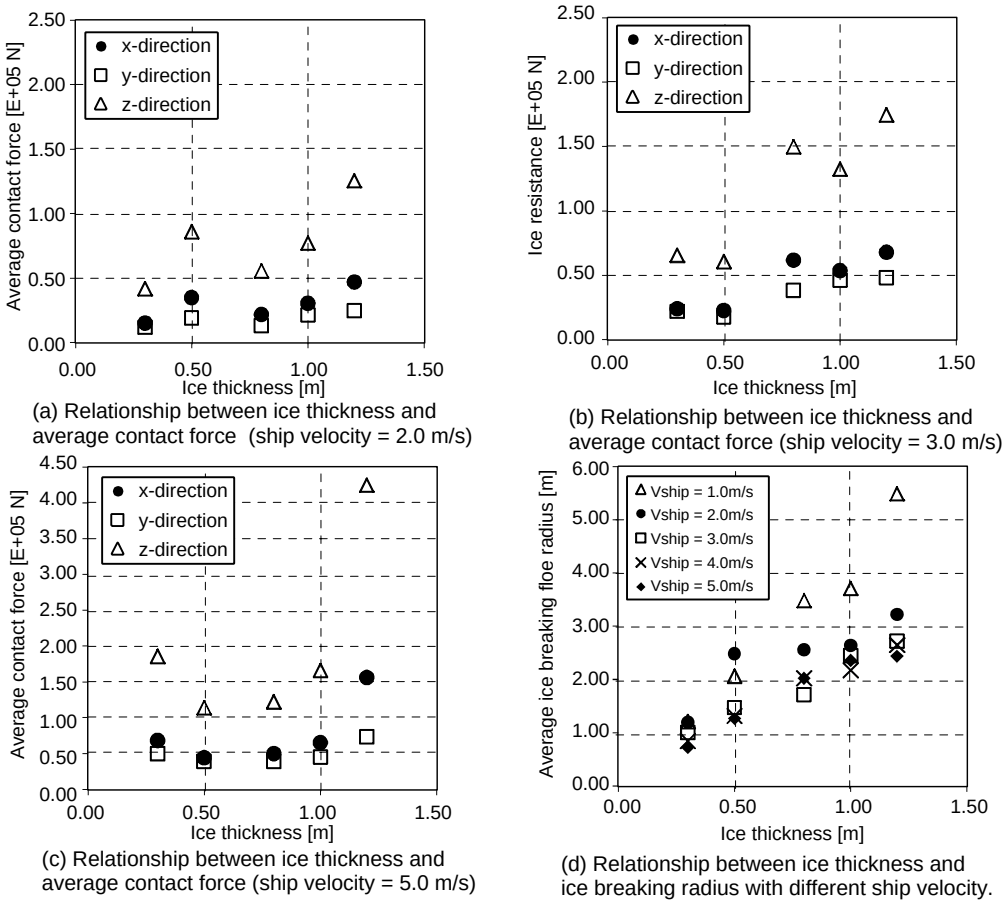

Figure 5. Relationship between ice thickness and average ice contact force (a-c) and the length of broken ice pieces (d) in different ship velocity.

Figure 6 illustrates the ice breaking pattern with different ice thickness at the ship speed = 3.0m/s. The widths of the breaking channel increase with increasing ice thickness which induces increase of the length of broken ice pieces as shown in Figure 5(d). However, the width of 0.8m ice thickness is relative larger than one of 1.0m thickness. This reason might be that, for ship maneuvering in the 0.8m thickness, the ice breaking with relative large length of the broken ice pieces occurs at the shoulder part where induces a large contact force. The shoulder contact might be reason that the irregular force peaks is induced in the conditions of 0.8m thickness and 3.0m/s ship speed.

Figure 7 illustrates the ice breaking pattern at different ship speeds with ice thickness = 0.5m. The widths of the breaking channel decrease with increasing ship speed which induces decrease of the length of broken ice pieces as shown in Figure 5(d). However, the width of 2.0m/s ship speed is almost same width as one of 1.0m/s ship speed. This reason can be explained by the same reason in the conditions of the ship speed = 3.0m/s and the ice thickness =0.8m, that is, the ice contacts occur at the shoulder which induce the large length of broken ice pieces. The average contact ice force strongly depends on the conditions of the ship and the ice. It's difficult to explain the relationship between the average force and ship-ice conditions by numerical results in this paper. We needs further investigations in different maneuvering conditions.

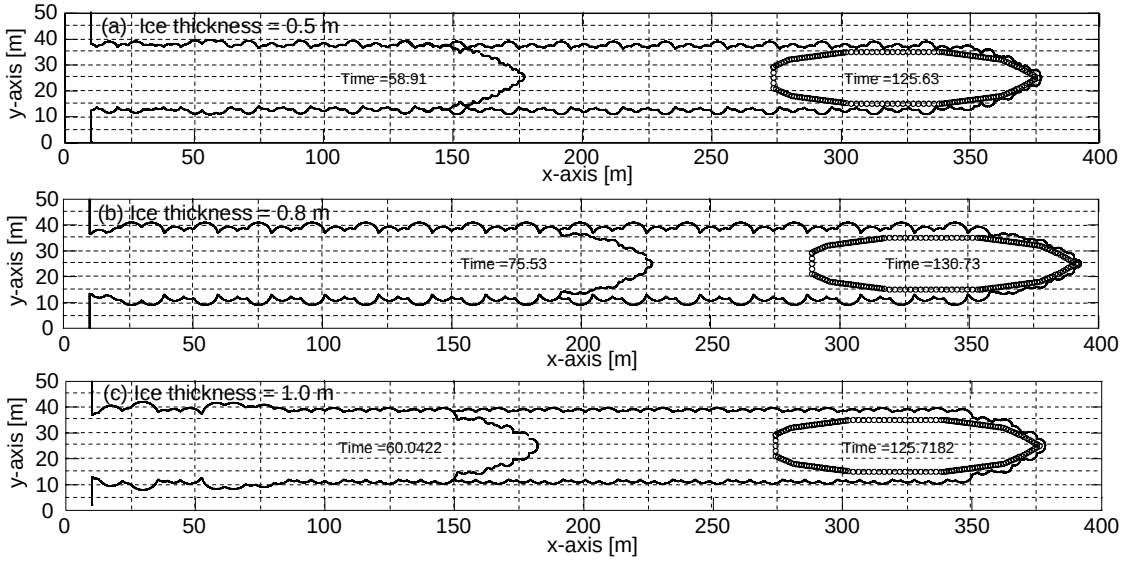

Figure 6. Ice breaking channel in ship maneuvering level ice with ship speed = 3.0m/s and ice thickness = 0.5, 0.8 and 1.0m.

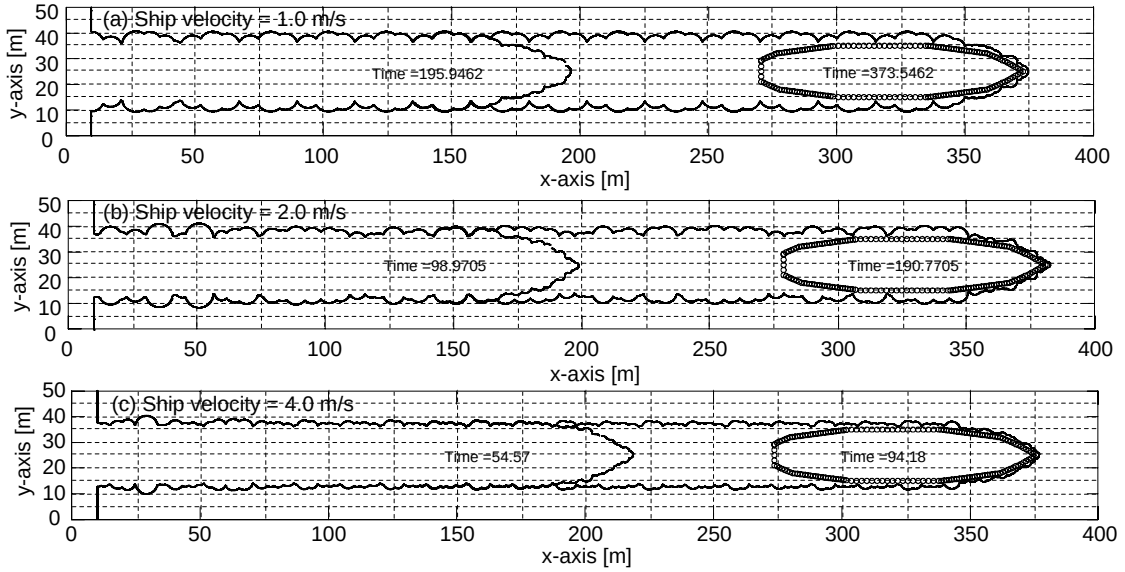

Figure 7. Ice breaking channel in ship maneuvering level ice with ice thickness = 0.5m and ship speed = 1.0, 2.0, and 4.0 m/s.

Ice force distribution in ship turning

The influence of a turning radius on the average ice contact force in x (surge), y (sway) and z (heave)-direction is investigated. A virtual icebreaker model with a sharp bow is used. Figure 8 shows the distributions of the average ice contact force and the average number of the ship-ice contacts along the waterline from the midship to the fore of the numerical model ship. In Figure 8, the ice breaking channels when the ship is turning at around 180° are shown. Turning radius R is 300, 500 and 800m. The ship speed v_s and the ice thickness h_i are 2.0m/s and 0.5m, respectively. The average ice force and the number of ship-ice contacts become quite higher distributions around the fore than the midship. Especially, z-direction force (bending component) becomes

significant. The hull form at fore has good icebreaking performance so that the ice plate is broken by the bending efficiently. In the inner side, the ice force and the ship-ice contact number is larger than outer side. These asymmetric distributions gradually are changing to symmetric ones with increasing the turning radius. In the small turning radius, the ice contacts around the midship occur so that relative larger ice forces in y-direction (compression component) are induced. The noticeable differences of ice breaking pattern between small and large turning radius cannot be observed.

The influence of a bow form on the average contact force is investigated. Figure 9 shows distributions of the average contact force, the average number of the ship-ice contacts and the ice breaking channel when the ship advances in the conditions of R=500m, v_s=2.0m/s and h_i=0.8m. The model ships with a sharp bow and the wide bow as shown in Figure 4 are used. The average contact force and the number of ship-ice contacts of the wide bow become remarkable high compared with the sharp bow. Moreover, in the case of the wide bow, the intense distributions of the average contact force at the fore are observed due to the concentration of the number of the ship-ice contacts at the fore. These distributions are quite different from one of the sharp bow. It is clear that the bow shape strongly affects the distribution of the ice load, namely, the ice resistance. In the wide bow, the small broken ice pieces are observed, and the relative complicated ice breaking channel is shown compared with one of the sharp bow.

CONCLUSION

This paper investigates the ice force distributions at the waterline when the ship advances straight forward and turns in a level ice. The numerical results show that the effect of the ice thickness, the ship speed, the turning radius and the bow shape on the average contact force is significant. The developed simulation can explain the relationship between the ice force distribution and the ship maneuvering conditions such as ice thickness and the ship speed. Therefore, the developed simulation has possibilities to understand ice load mechanism. However, in order to verify our developed numerical simulation, the results of the simulations have to be compared with the model tests or the full-scaled data.

ACKNOWLEDGEMENT

This research was supported by the KAKENHI (22760633) and the Shipbuilders' Association of Japan (SAJ).

REFERENCES

Izumiyama, K, Wako, D. and Uto, S., 2001. Ice Pressure Acting over a Model Ship Hull. Proceeding of the 16th International Conference on Port and Ocean Engineering under Arctic Conditions, Vol. 2, pp. 793-802

Kayo, Y., 1993. Measurement of Ice Load Distribution on the Icebreaker Bow Model. Proceeding of the 12th International Conference on Port and Ocean Engineering under Arctic Conditions, Vol. 1, pp. 328-337

Likkonen, S. and Nortala-Hoikkanen, A., 1992. Ice Pressure Test on a Segmented Ice Breaker Model. Proceeding of the International Symposium on Ice, vol. 1, pp. 296-308

Liu J.C., Lau M. and Williams F. M., 2008. Numerical Implementation and Benchmark of Ice-Hull Interaction Model for Ship Maneuvering. 19th IAHR International Symposium on Ice, pp.165-176

Sawamura, J., Riska, K. and Moan T., 2008. Finite Element Analysis of Fluid-Ice Interaction during Ice Bending" The proceedings of 19th IAHR International Symposium on Ice, pp.191-132
Sawamura, J., Tsuchiya, H., Tachibana, T. and Osawa, N., 2010. Numerical Modeling for Ship Maneuvering in Level Ice. Proceeding of the 20th IAHR International Symposium on Ice, No64

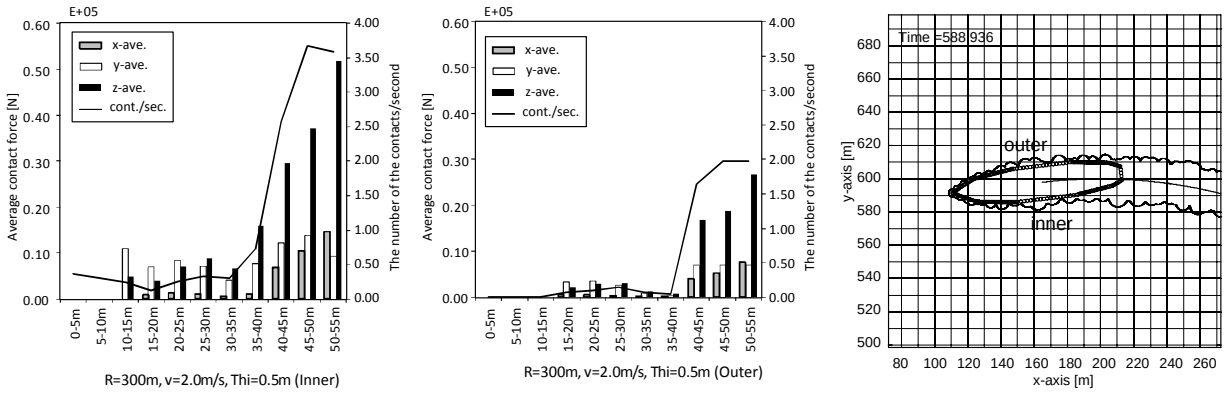

(a) Distributions of Ice contact force and the number of the ship-ice contacts at the waterline (Left: inner, Center: outer) and ice breaking channle (Right) in ship turning R=300m

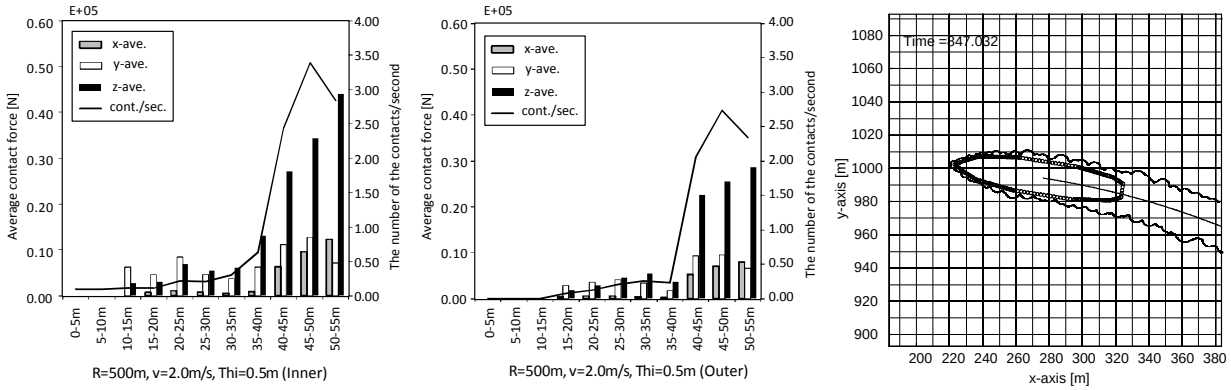

(b) Distributions of Ice contact force and the number of the ship-ice contacts at the waterline (Left: inner, Center: outer) and ice breaking channle (Right) in ship turning R=500m

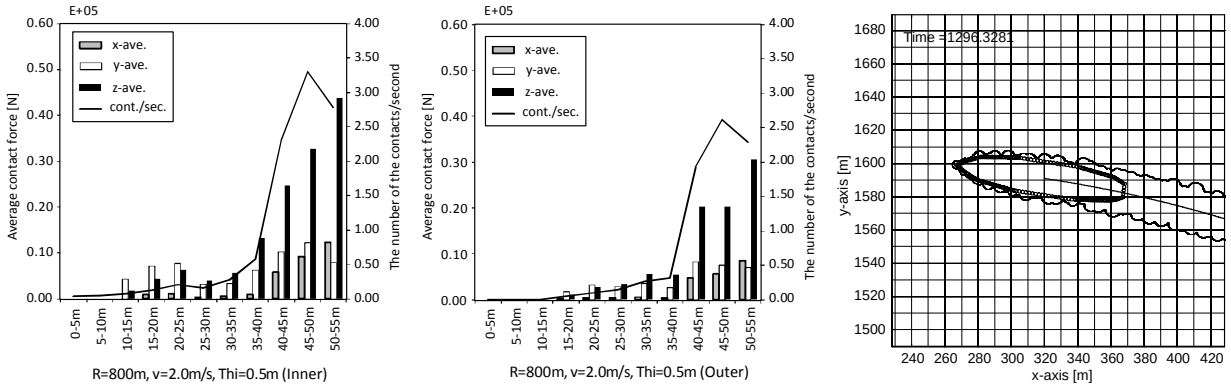

(c) Distributions of Ice contact force and the number of the ship-ice contacts at the waterline (Left: inner, Center: outer) and ice breaking channle (Right) in ship turning R=800m

Figure 8. Distributions of the average ice force, the average number of ship-ice contacts at the waterline from the midship to the fore and ice breaking channel in difference turning radius R=300, 500, and 800m. (Ship speed = 2.0m/s, Ice thickness = 0.5m)

Valanto, P., 2009. On Computed Ice load Distributions, Magnitude and Lengths on Ship Hulls Moving in Level Ice. Proceeding of the 20th International Conference on Port and Ocean Engineering under Arctic Conditions, No 90.

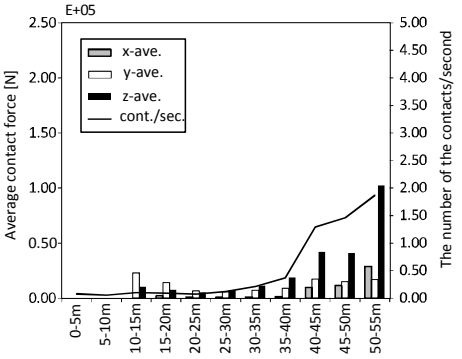

(a-1) R=500m, v=2.0m/s, Thickness=0.8m (Inner)

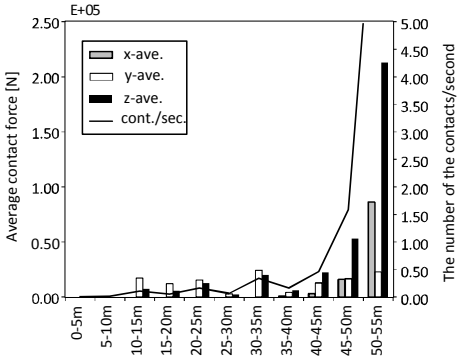

(b-1) R=500m, v=2.0m/s, Thickness=0.8m (Inner), Wide bow

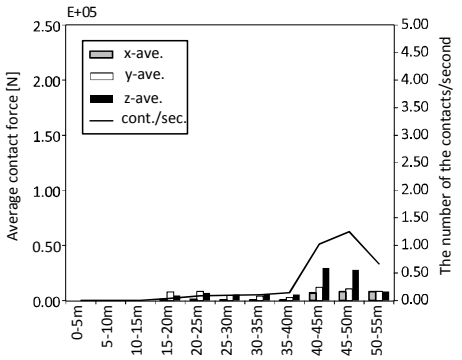

(a-2) R=500m, v=2.0m/s, Thickness=0.8m (Outer)

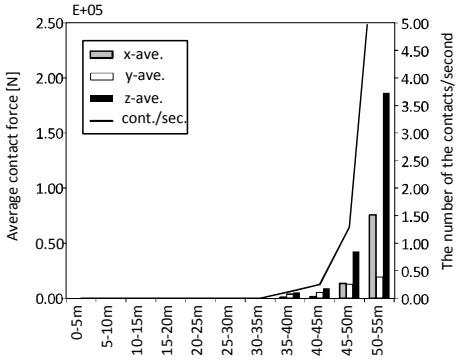

(b-2) R=500m, v=2.0m/s, Thickness=0.8m (Outer), Wide bow

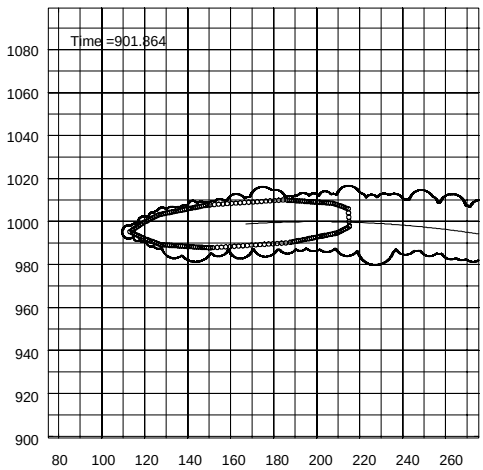

(a-3) Ice breaking channle with R=500m, v=2.0m/s, Thickness=0.8m (time=901s. rotate=183deg.)

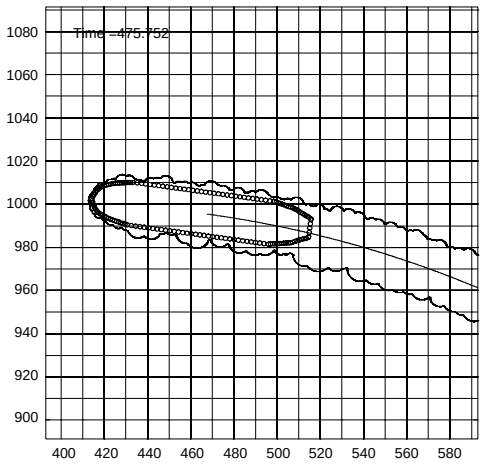

(b-3) Ice breaking channle with R=500m, v=4.0m/s, Thickness=0.8m (time=475s. rotate=172deg.)

(a) Distributions of Ice contact force and the number of the ship-ice contacts at the waterline (Top: inner, Middle: outer) and ice breaking channle (Bottom) with a sharp bow.

(b) Distributions of Ice contact force and the number of the ship-ice contacts at the waterline (Top: inner, Middle: outer) and ice breaking channle (Bottom) with a wide bow.

Figure 9. Comparison of average ice force, the average number of ship-ice contacts at the waterline and ice breaking channel between the sharp bow and the wide bow. (Ship speed = 2.0m/s, Ice thickness = 0.5m, Turning radius = 500m)